

Supplementary Material

Surface engineering of $\text{Li}_3\text{V}_2(\text{PO}_4)_3$ -based cathode materials with enhanced performance for lithium-ion batteries working in a wide temperature range

Minxia Liang^{1,2,#}, Yiting Wang^{1,2,#}, Hanghang Dong^{1,4}, Lei Wang², Qianqian Peng², Chao Yang², Yao Xiao¹, Yong Wang², Shulei Chou¹, Bing Sun³, Shuangqiang Chen^{1,2}

¹Institute for Carbon Neutralization, College of Chemistry and Materials Engineering, Wenzhou 325035, Zhejiang, China.

²Department of Chemical Engineering, School of Environmental and Chemical Engineering, Shanghai University, Shanghai 200444, China.

³Centre for Clean Energy Technology, School of Mathematical and Physical Sciences, Faculty of Science, University of Technology Sydney, Ultimo, NSW 2007, Australia.

⁴School of Energy and Power Engineering, Nanjing University of Science and Technology, Nanjing 210094, Jiangsu, China.

#Authors contributed equally.

Correspondence to: Prof. Shuangqiang Chen, Institute for Carbon Neutralization, College of Chemistry and Materials Engineering, Wenzhou University, No. 77 Fengdong Road, Wenzhou 325035, Zhejiang, China. E-mail: chensq@shu.edu.cn; Dr. Bing Sun, Centre for Clean Energy Technology, School of Mathematical and Physical Sciences, Faculty of Science, University of Technology Sydney, 15 Broadway, Ultimo, NSW 2007, Australia. E-mail: bing.sun@uts.edu.au; Dr. Hanghang Dong, Department of Chemical Engineering, School of Environmental and Chemical Engineering, Shanghai University, Shangda Road 99, Shanghai 200444, China. E-mail: donghangh@njust.edu.cn

MATERIALS AND METHODS

Synthesis of LVP@NC-x (x = 0.5, 0.8, 1, 2, and 3)

LVP@NC-x materials were synthesized using $\text{H}_2\text{C}_2\text{O}_4 \cdot 2\text{H}_2\text{O}$, Li_2CO_3 , V_2O_5 , $\text{NH}_4\text{H}_2\text{PO}_4$, and STAB as raw materials (molar ratio: oxalic acid: Li: V: P: STAB = 3: 3: 2: 3: x) by hydrothermal assisted sol-gel method. $\text{H}_2\text{C}_2\text{O}_4 \cdot 2\text{H}_2\text{O}$ and V_2O_5 were added to distilled water at 80 °C and then stirred

continuously. Next, the mixed solution of Li_2CO_3 and $\text{NH}_4\text{H}_2\text{PO}_4$ was added to the above solution, followed by the STAB solution. After stirring at $80\text{ }^\circ\text{C}$ for 1 h, the mixtures were transferred into the Teflon-lined steel autoclave and kept at $180\text{ }^\circ\text{C}$ for 24 h. After that, the distilled water was evaporated by a Sol-Gel method. The obtained gel precursors were further dried in a vacuum oven at $80\text{ }^\circ\text{C}$, followed by calcination at $750\text{ }^\circ\text{C}$ for 6 h in H_2 : Ar (5: 95 *vol.*%) to obtain nitrogen-doped carbon-network coated $\text{Li}_3\text{V}_2(\text{PO}_4)_3$. In addition, $\text{Li}_3\text{V}_2(\text{PO}_4)_3$ -based materials with different nitrogen-doped carbon content were obtained by adding the different content of STAB, named LVP@NC-x (x = 0.5, 0.8, 1, 2, and 3).

Characterization of materials

XRD investigation was performed to investigate the crystallographic information, and *in-situ* XRD was used to observe the phase changes during the electrochemical reactions using a Bruker D8 Advance X-ray diffractometer with Cu K_α X-Ray source. SEM images were collected with a Hitachi SU1510 scanning electron microscope. TEM images were recorded by a Hitachi-7500 transmission electron microscope. FTIR spectra were obtained using a Nicolet iS50 FTIR spectrometer. The properties of the carbon coating layer were analyzed by a Renishaw inVia Raman microscope. BET surface area was measured using micromeritic ASAP 2460 equipment. The surface compositions of the materials were evaluated by a Thermo Scientific K-Alpha X-ray photoelectron spectrometer.

Electrochemical measurements

Electrochemical performances of all samples were evaluated with standard CR2032 coin cells, in which lithium foil was used as the reference and counter electrode for half-cell and graphite as the anode for full cell, with polypropylene film (Celgard 2400) as the separator. Recipe LB-111 (the main component was LiPF_6 dissolved in ethylene carbon (EC) and dimethyl carbonate (DMC)) was purchased from DoDoChem. Technology Co., Ltd. as the electrolyte. The working electrodes were fabricated with active material, Ketjen Black, and polyvinylidene difluoride (PVDF) with a weight ratio of 7:2:1. The mixtures were pasted on Al foils and then punched into circular discs with a diameter of 12 mm. The cells were assembled in a glove box filled with pure argon. Galvanostatic

charge/discharge measurements were studied in a voltage range of 3.0-4.8 V vs. Li/Li⁺ at different temperatures on the multichannel battery testing system (NEWARE CT-4008T) in temperature-controlled test chambers (BPHJS 060B). Cyclic voltammetry (CV) tests were performed on an electrochemical workstation (LANHE G340A). Electrochemical impedance spectroscopy (EIS) was performed using an electrochemical workstation (Zahner Zennium E) in the frequency range of 10 kHz to 10 mHz.

The electrochemical performances of LVP@NC-0.8 || graphite full cell were tested at room temperature. The LVP@NC-0.8 cathode and graphite anode were first tested in three cycles in the form of half-cell at 0.5 C to reach the steady state. The capacity ratio (~1:1.9) of the cathode and anode results in the mass load of 0.37 mg cm⁻² and 0.7 mg cm⁻² for the cathode and anode, respectively.

Calculation of D_{Li⁺}

Galvanostatic intermittent titration technique (GITT) measurements were performed on a multichannel battery testing system (LAND CT3001A). GITT is a common method to determine the diffusion coefficient of lithium ions (D_{Li⁺}) calculated *via* Fick's second diffusion law. The calculation equation of the D_{Li⁺} is as below^[1]:

$$D_{Li^+} = \frac{4}{\pi\tau} \left(\frac{m_B V_M}{M_B S} \right)^2 \left(\frac{\Delta E_s}{\Delta E_t} \right)^2 \quad \left(\tau \ll \frac{L^2}{D_{Li^+}} \right) \quad (1)$$

In this equation, τ (s) is the titration time. m_B is the mass of the active material. M_B and V_M are the molar weight and the molar volume of the compound, respectively. S is the surface area between the electrode and the electrolyte. ΔE_s is the change of voltage during charge/discharge. ΔE_t is the difference of two consequent stabilized open circuit voltages. And L is the thickness of the electrode. In calculations, it is assumed that the molar volume (V_M) remains stable during both the charge and discharge processes, and the possible change in it is ignored.

DFT theoretical calculations

All calculations were performed by DFT using the Cambridge Sequential Total Energy Package Code (CASTEP) function of Material Studio software. The exchange-correlation function was the spin-polarized generalized gradient approximation (GGA) of Perdew-Burke-Ernzerhof (PBE)^[2, 3]. The on-

site Coulomb U_{eff} values for V were set to be 4.2 eV in the present work according to the previous reference^[4]. The Brillouin zone integrals were sampled using a $2 \times 2 \times 1$ K-point grid for geometric optimization^[5]. Geometry optimization was carried out by relaxing all atomic positions until the interatomic force was less than 0.02 eV \AA^{-1} . A smearing value of 0.05 eV was adopted to accelerate the convenience. In addition, the lithium migration paths, and the corresponding energy barriers were calculated by the nudged elastic band (NEB) method.

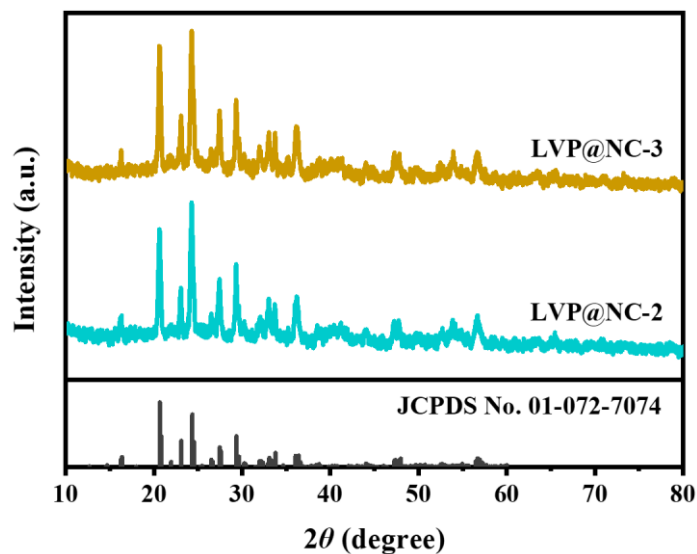


Figure S1. XRD patterns of LVP@NC- x ($x = 2$ and 3) composites.

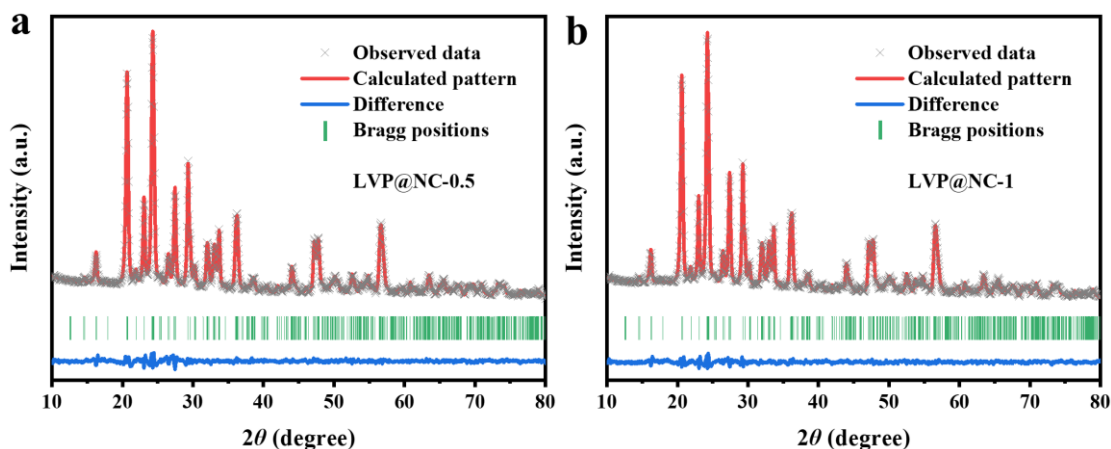


Figure S2. Rietveld refinement of (a) LVP@NC-0.5 and (b) LVP@NC-1 composites.

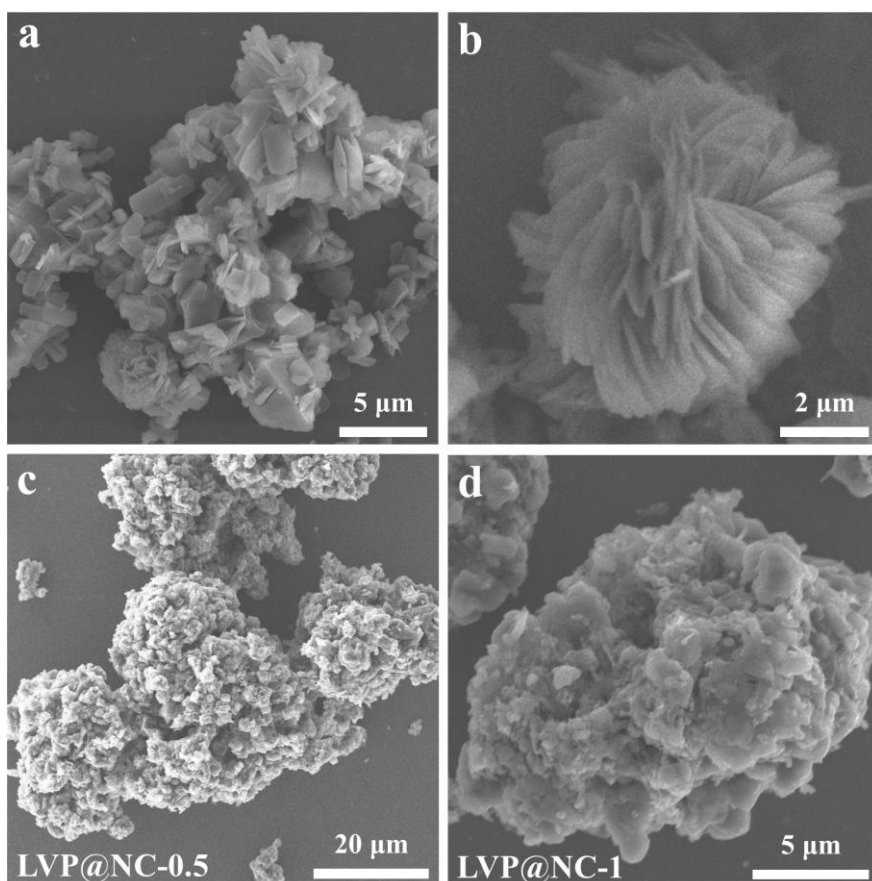


Figure S3. SEM images of (a, b) precursors and (c, d) composites of (a, c) LVP@NC-0.5 and (b, d) LVP@NC-1.

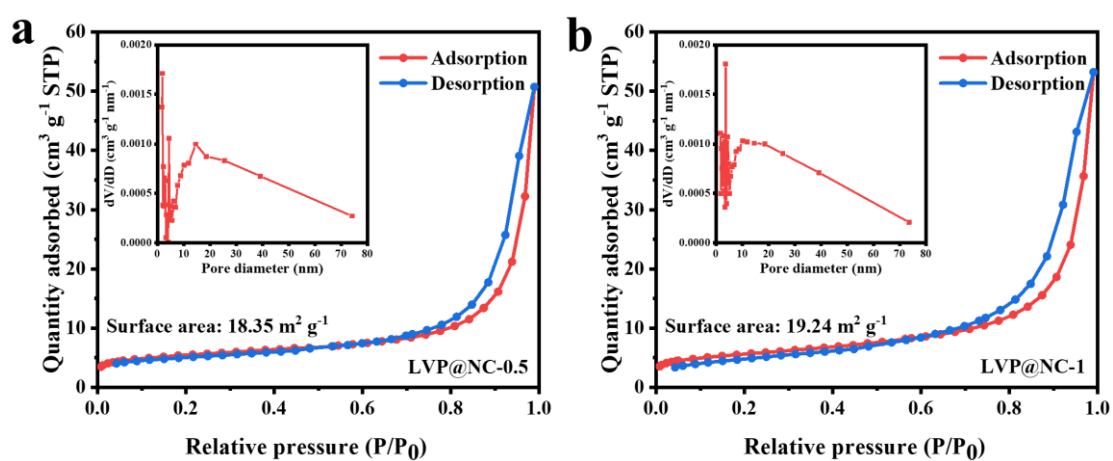


Figure S4. Nitrogen adsorption-desorption isotherms of (a) LVP@NC-0.5 and (b) LVP@NC-1 composites, the inset is the corresponding pore size distribution curve.

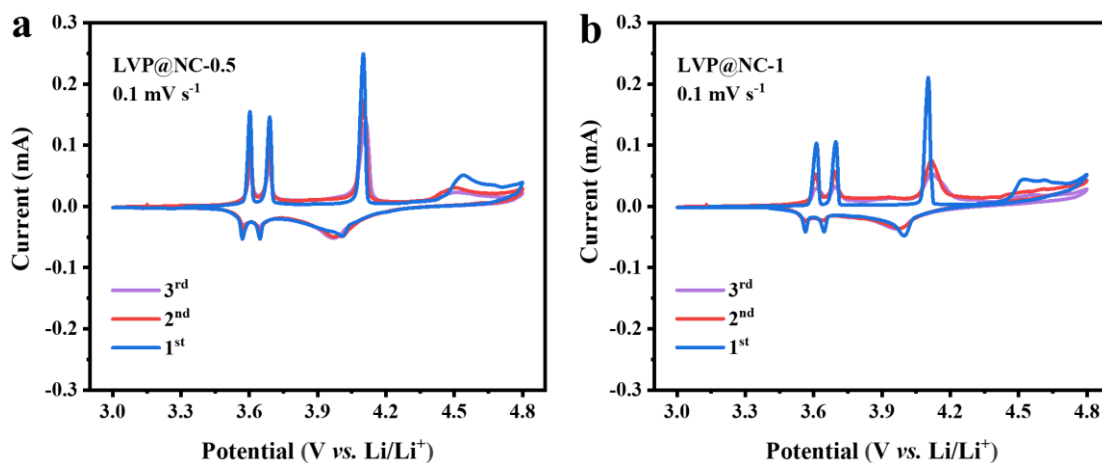


Figure S5. The first three CV curves at 0.1 mV s^{-1} of (a) LVP@NC-0.5 and (b) LVP@NC-1.

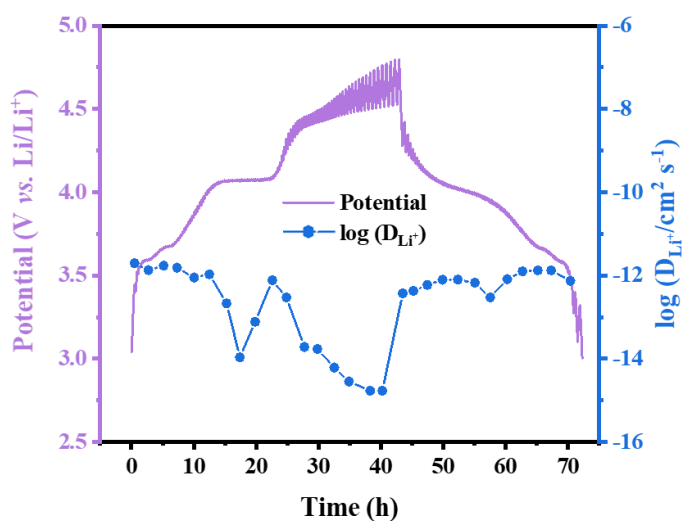


Figure S6. The GITT curves and calculated lithium-ion diffusion coefficients of LVP@NC-0.8 composite.

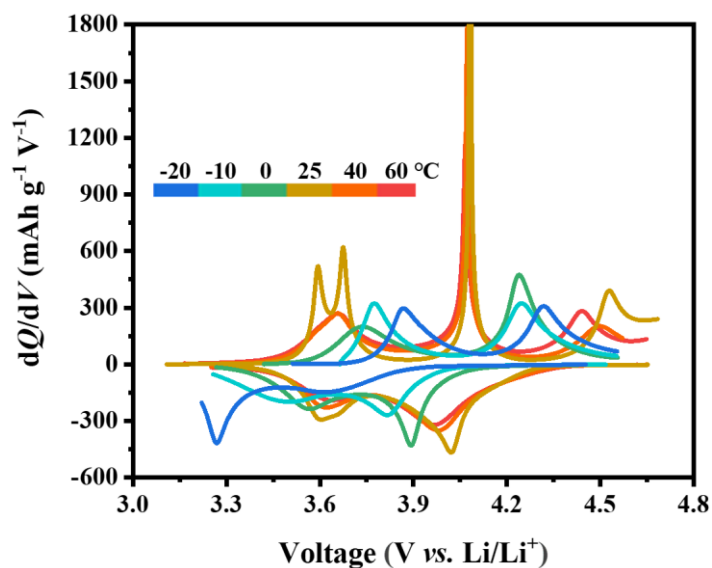


Figure S7. The dQ/dV profiles of LVP@NC-0.8 electrode at different temperatures at 0.5 C.

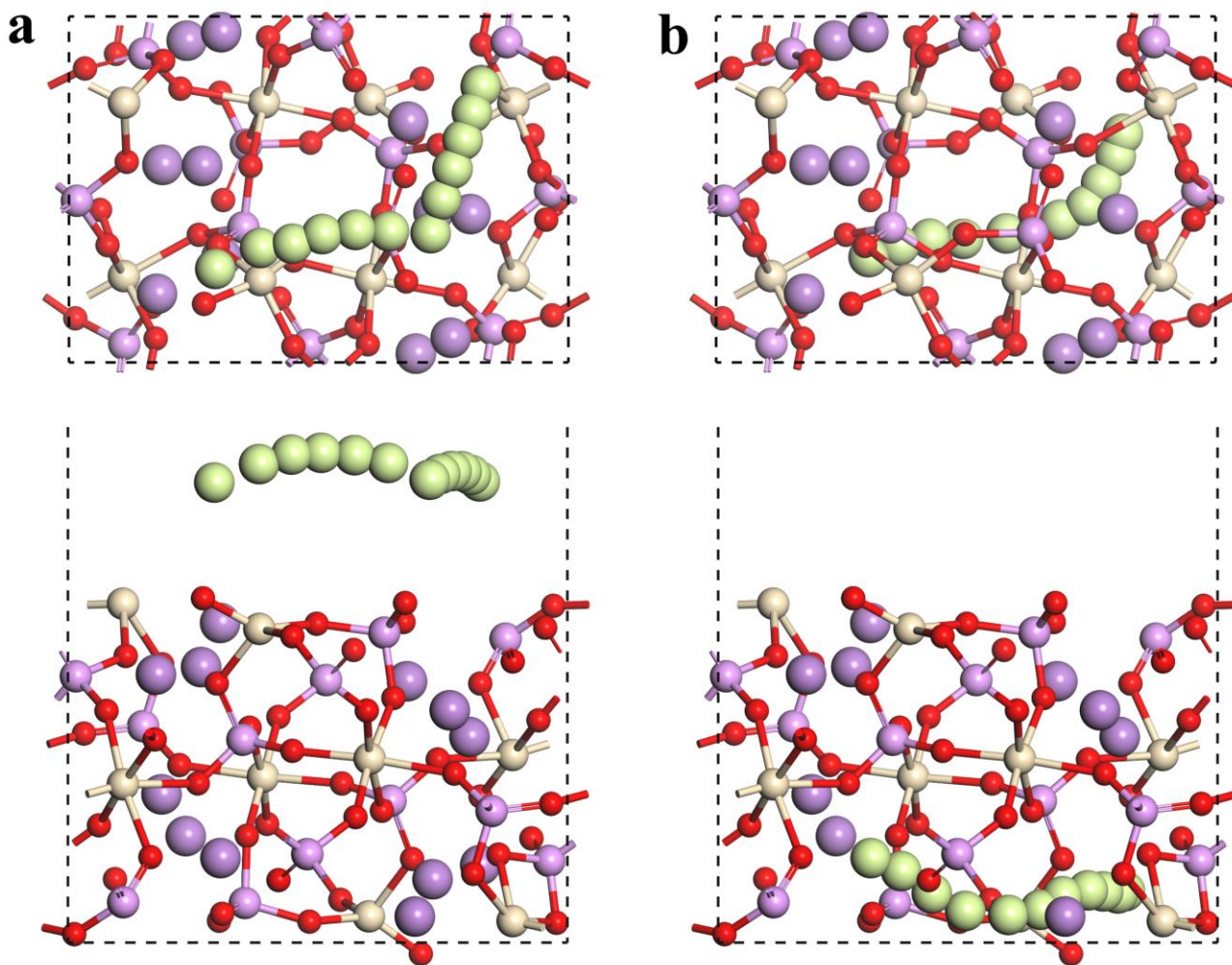


Figure S8. Schematics of the possible migration pathway of lithium-ion (a) outside pure LVP and (b) in pure LVP subject. In addition, the yellow, brown, purple, and red spheres in cells represent Li, V, P, and O atoms, respectively.

Table S1. The refined lattice parameters and Rietveld refinement factors of LVP@NC-x (x = 0.5, 0.8, and 1) composites.

Composite	<i>a</i> (Å)	<i>b</i> (Å)	<i>c</i> (Å)	β (°)	<i>V</i> (Å ³)	<i>R</i> _{wp} %	<i>R</i> _{exp} %
LVP@NC-0.5	8.6167054	8.6119798	12.0597900	90.51672	894.88315	1.836	2.92
LVP@NC-0.8	8.6126348	8.6090336	12.0559484	90.52203	893.86881	1.857	2.89
LVP@NC-1	8.6189755	8.6110900	12.0641162	90.55871	895.34133	1.623	2.80

Table S2. The element content of N and C in all composites by elemental analysis.

Sample	N (%)	C (%)
LVP@NC-0.5	0.24	2.87
LVP@NC-0.8	0.22	3.41
LVP@NC-1	0.27	4.01

Table S3. The fitted values of *R*_s and *R*_{ct} of LVP@NC-x (x = 0.5, 0.8, and 1) composites.

Composite	<i>R</i> _s (ohm)	<i>R</i> _{ct} (ohm)
LVP@NC-0.5	7.079	113.8
LVP@NC-0.8	8.469	97.41
LVP@NC-1	7.720	131.8

Table S4. Compared results of as-prepared LVP@NC-0.8 and other reported cathode materials.

Cathode material	Temperature (°C)	Capacity (mAh g ⁻¹)	Reference
Trace Al surface-doped LiNi _{0.5} Co _{0.2} Mn _{0.3} O ₂	-20	106.1 (1 C)	[6]
LTO-coated LiMn ₂ O ₄	60	134.9 (0.2 C)	[7]
LiMn _{1.5} Ni _{0.5} O _{3.8} F _{0.2}	60	~120 (44 mA g ⁻¹)	[8]
Nano-LiFePO ₄	-20	111.8 (0.5 C)	[9]
LVP@NC-0.8	60	156 (0.5 C)	This work
LVP@NC-0.8	-20	119 (0.5 C)	This work

REFERENCES

1. Rui, X. H., Ding, N., Liu, J., Li, C., Chen, C. H. Analysis of the chemical diffusion coefficient of lithium ions in Li₃V₂(PO₄)₃ cathode material. *Electrochim Acta* 2010; 7: 2384-90. DOI: 10.1016/j.electacta.2009.11.096.
2. Perdew, J. P., Wang, Y. Accurate and simple analytic representation of the electron-gas correlation energy. *Phys Rev B Condens Matter* 1992; 23: 13244-49. DOI: 10.1103/physrevb.45.13244.
3. Vanderbilt, D. Soft self-consistent pseudopotentials in a generalized eigenvalue formalism. *Phys Rev B Condens Matter* 1990; 11: 7892-95. DOI: 10.1103/physrevb.41.7892.
4. Ni, Q., Zheng, L., Bai, Y., Liu, T., Ren, H., et al. An extremely fast charging Li₃V₂(PO₄)₃ cathode at a 4.8 V cutoff voltage for Li-ion batteries. *ACS Energy Lett.* 2020; 6: 1763-70. DOI: 10.1021/acsenerylett.0c00702.
5. Setyawan, W., Curtarolo, S. High-throughput electronic band structure calculations: challenges and tools. *Comp Mater Sci* 2010; 2: 299-312. DOI: 10.1016/j.commatsci.2010.05.010.
6. Li, G., Zhang, Z., Wang, R., Huang, Z., Zuo, Z., et al. Effect of trace Al surface doping on the structure, surface chemistry and low temperature performance of LiNi_{0.5}Co_{0.2}Mn_{0.3}O₂ cathode. *Electrochim Acta* 2016: 399-407. DOI: 10.1016/j.electacta.2016.07.033.
7. Li, J., Zhu, Y., Wang, L., Cao, C. Lithium titanate epitaxial coating on spinel lithium manganese oxide surface for improving the performance of lithium storage capability. *ACS Appl Mater Interfaces* 2014; 21: 18742-50. DOI: 10.1021/am504319y.

8. Hagh, N. M., Amatucci, G. G. Effect of cation and anion doping on microstructure and electrochemical properties of the $\text{LiMn}_{1.5}\text{Ni}_{0.5}\text{O}_{4-\delta}$ spinel. *J Power Sources* 2014: 457-69. DOI: 10.1016/j.jpowsour.2013.12.135.
9. Zheng, F., Yang, C., Ji, X., Hu, D., Chen, Y., et al. Surfactants assisted synthesis and electrochemical properties of nano- LiFePO_4/C cathode materials for low temperature applications. *J Power Sources* 2015: 337-44. DOI: 10.1016/j.jpowsour.2015.04.126.